Peak Strength Analysis and Failure Process Simulation of Brittle Materials with an Open-hole under Uniaxial Compression

by

Cheng ZHAO*, Hiroshi MATSUDA**, Mei HUANG**,

Hayato KOUZUMA*** and Hirosachi KAWABAYASI***

Present paper consists of peak strength model and failure process simulation of both experimental and numerical method. The peak strength model of brittle materials with a pre-existing open-hole defect is proposed in this paper. A modified Sammis-Ashby model is deduced, which can be used to calculate the peak strength of brittle materials. It shows the law between peak strength σ and independent variable μ, which is the ratio of open-hole radius (a) to half-width of the specimen (t). Then in the second part, both of experimental and numerical investigations were carried on open-hole specimens. A progressive elastic damage method (RFPA) is employed to inspect and verify the modified model and simulation the failure process. The investigation finds that there are good correlations between the experimental and numerical values. In the process simulation, due to the influences of boundary conditions, secondary cracks developed in the shear zones till failure, therefore the shear failure type was obtained.

Key words: *Peak strength, Brittle materials, Open-hole, Numerical test, Failure process*

NOMENCLATURE

E_0	specimen's Young's modulus	μ	ratio of a/t
λ	ratio of σ_3/σ_1	K_{IC}	fracture toughness
α	a constant (0.55 in this study)	l	the length of the secondary crack
a	radius of an open-hole	L	normalised crack length
t	half-width of the specimen	G	crack-extension force
γ	surface energy per unite area		

1. INTRODUCTION

Structural materials especially concrete or other brittle materials, they usually contain some pre-existing defects, either because of the making process of materials themselves or due to the requirements of structures, for example the structural components may need to be weakened according to the utility pipelines and other realistic functions. When they are loaded in compression, those secondary failures are always determined by these pre-existing defects, and finally they have great effects on the whole failure. In order to clarify the effect of defects on concrete structural and other brittle materials, the plate specimen was chosen. Because in present methods to obtain the inside crack paths are not so accurate or acceptable, by using the plate specimen, secondary cracks can easily occur and develop on the surface, therefore this study was carried out. Although the mechanics of brittle failure of solids containing open-hole defects has been a subject of intensive research for many years [1],

Received on Jun. 27, 2008

* Graduate School of Science and Technology

** Department of Structural Engineering

*** Graduate School of Science and Technology

there is no standard on the experiment of plates of concrete or other artificial materials containing holes. Such theoretical analysis is also rarely carried out [2]. Because of their complexity, such experimental tests are seldom carried out too [3]. Failure of this type is most generally observed in solid laboratory samples (Jaeger and Cook, 1976; Holzhausen and Johnson, 1979). The pre-existing open-hole can interact with a compressive stress field in a way which causes new cracks to grow from it. If these cracks extend to the specimen's surface, or if they interact with each other so that they grow unstably, then a macroscopic failure may follow [3].Because the type of failure highly depends upon the confining pressure [4], in order to get the uniform fracture type, uniaxial compression analysis is carried out in this analysis, in which $\sigma_3=0$.

In Sammis and Ashby's experiments (1986), plate specimens containing a single hole of the same size or an array of holes with various diameters were tested. The purpose of their experiments is to investigate the interaction of growing cracks with the surfaces of the specimen and the interaction with secondary cracks themselves. The experimental results show that cracks initiated from the holes interact with the surfaces of the finite specimen in a way that causes them to grow longer than they do in an infinite medium. Based on Sammis and Ashby theoretical crack model [5], the modified formulation for calculating the peak strength of brittle specimens with an open-hole is deduced in this study. This paper also presents a series of numerical test results of uniaxial compression. Test samples contain single hole with varied diameters and the sample widths are also changed for two types. The theoretical peak strength of brittle materials and the numerical values are also compared and discussed in this paper.

2. SAMMIS-ASHBY`S THEORY

In Sammis and Ashby's research, they analyzed the growth of a crack from a circle hole with the radius a, contained in a plate subjected to a remote biaxial stress field (σ_1, σ_3), as shown in Fig.1.

The hole in an infinite plate is considered first; then the interaction of the growing crack with the edges of a finite plate is analyzed, it can be completely divided into two steps:

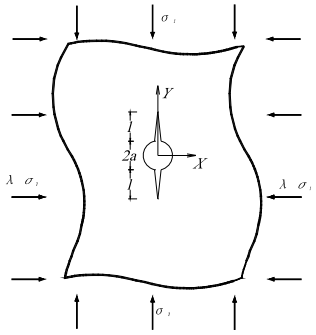

Fig.1 Crack geometry and co-ordinate system in an infinite plate

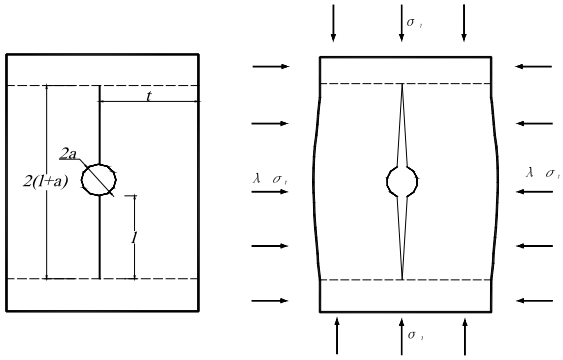

a. Diagram of a finite plate with an open-hole b. The bending displacement and associated cracks

Fig.2 Schematic of a finite plate containing a open-hole under loading

2.1 Crack growth from a hole in an infinite plate

Sammis and Ashby Considered an elastic plate containing an open-hole of radius a and subjected to principal stresses σ_1 and σ_3. The stresses are treated as positive when tensile and negative when compressive. By setting the ratio of σ_3/σ_1 as λ, according to the Appendix of referenced paper [4], the equation as follows is deduced:

$$F(\lambda, L) \cong \frac{1.1(1-2.1\lambda)}{(1+L)^{3.3}} - \lambda \qquad (1)$$

From which

$$K_{IC} = -\sigma_1 \sqrt{\pi a} L^{1/2} \left[\frac{1.1(1-2.1\lambda)}{(1+L)^{3.3}} - \lambda \right] \qquad (2)$$

2.2 Interaction of the cracks with the surface

Sammis and Ashby's research shows that the cracks grow in the way described by equation (2) when they are short and the plate containing them is

large, but that they extended much further than this when l (the length of secondary cracks) becomes comparable with the plate width 2t as shown in Fig.2[2]. Considering the interaction of the micro-cracks during extending, they got equation (3) as follows to determine the stress intensity:

$$K_I^B = -\left(\frac{3}{\pi}\cdot\frac{a}{t}\right)^{0.5}\frac{\alpha^2}{1+L}\sigma_1\sqrt{\pi r}\cdot\left[\frac{1-\frac{2}{3}\cdot\frac{(1+L)^3}{\alpha^2}\cdot\frac{a}{t}\cdot\lambda}{1+\frac{12}{\pi^2}\cdot\frac{\sigma_1}{E_0}\cdot\frac{a^2}{t^2}(1+L)^2}\right] \quad (3)$$

Sammis and Ashby's experiments shows that K_I^B is negligible for wide plate ($t/a \gg 1$), but becomes increasingly important as t/a approaches 1[2].

3. MODIFIED MODEL

Since the deduction is based on uniaxial compression test and the specimens follows the failure mode I (tension crack mode), for the uniaxial loading $\sigma_3 = 0$, which means $\lambda = \sigma_3/\sigma_1 = 0$. So the equation (2) is given by

$$K_I = -\sigma_1\sqrt{\pi a}\left[\frac{1.1\sqrt{L}}{(1+L)^{3.3}}\right] \quad (4)$$

In which L (normalized crack length) can be determined either from the laboratory test or numerical test. And it is simply defined by $L = l/a$ (l is the length of the crack and a is the radius of open-hole). The crack grows until the stress intensity K_I becomes equal to the fracture toughness K_{IC}.

By setting $\mu = a/t$, meanwhile because of $\lambda = 0$, equation (3) is given by:

$$K_I^B = -\sqrt{\frac{3}{\pi}\cdot\mu}\,\frac{\alpha^2}{1+L}\sigma_1\sqrt{\pi a}\left[\frac{1}{1+\frac{12}{\pi^2}\cdot\frac{\sigma_1}{E_0}\cdot\mu^2(1+L)^2}\right] \quad (5)$$

In which E_0 is the brittle materials' Young's Modulus, α a constant of effective hole-depth, it is mainly depended on the material itself. Sammis and Ashby found that for $\alpha = 0.6$, it gives the best correspondence between theoretical and experimental values [5]. In this deduction $\alpha = 0.55$ is employed. (Culled from referenced paper [6].)

Before the loading reaches the peak strength, the fracture toughness K_{IC} must be attained. Here K_{IC} contains two parts which is the one for cracks growth and the other for calculating the interaction of the cracks during their developing. Which are shown in equation (4) and (5). When the specimen failed which means:

$$\sigma_1 = \sigma_p \quad (6)$$

Here σ_p is the peak strength of the specimens with an open-hole. It is treated as positive when tensile, negative when compressive.

Then the fracture toughness of the whole specimen with an open-hole is setting:

$$K_{IC} = K_I + K_I^B \quad (7)$$

From which

$$K_{IC} = -\left\{\frac{1.1\sqrt{L}}{(1+L)^{3.3}} + \sqrt{\frac{3}{\pi}\mu}\cdot\frac{\alpha^2}{1+L}\cdot\left[\frac{1}{1+\frac{12}{\pi^2 E_0}\cdot\mu^2(1+L)^2\sigma_p}\right]\right\}\sigma_p\sqrt{\pi a} \quad (8)$$

By setting:

$$A = \frac{1.1\sqrt{L}}{(1+L)^{3.3}} \quad (9)$$

$$B = \frac{12(1+L)^2}{\pi^2 E_0} \quad (10)$$

$$\text{and } C = \frac{\alpha^2}{1+L} \quad (11)$$

The equation (8) is given by:

$$K_{IC} = -\left(\sqrt{\pi a}A\cdot\mu^2 B\right)\sigma_p^2 - \left(\sqrt{\pi a}A + K_{IC}\mu^2 B + \sqrt{3a\mu}C\right)\sigma_p \quad (12)$$

Because of L, α and E_0 are depend on the materials` properties, they would be constants, which means A, B and C in equations above are constants for this research too. In equation (12), σ_p is the

peak strength of brittle specimens with open-hole defect and $\mu = a/t$ shows the degree of imperfection for an integral specimen. The equation shows us not only the correspondence between σ_p and μ, but also the geometry effect of the specimens by containing the factor of $\sqrt{\pi a}$. That is much more acceptable when calculating the peak strength.

The analysis of the fracture toughness K_{IC} is evaluated based on the calculating of the elastic energy. By giving the crack-extension force G, K_{IC} can be done by the relationship of equation (13).

$$(K_{IC})^2 = EG = 2E\gamma \tag{13}$$

In which γ is the surface energy per unite area [5]. As many researchers have done lots on the studied, most of the popular theories about it are also based on the experimental analysis [7] [8]. In our study, we used SENRB method to calculate the fracture toughness K_{IC}. Detail about this method was filed by R.H.Wong [9]. By using it, the fracture toughness can be determined by the numerical test, so that peak strength can be obtained according to equation (11). Test method is shown in Fig.3.

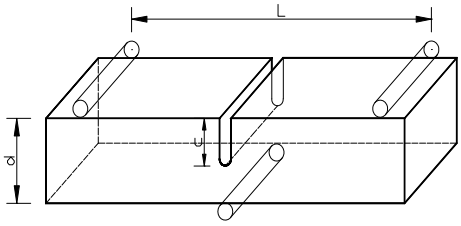

Fig.3 Schematic of three points test method

The fracture toughness can be calculated by follow equation (13) [9].

$$K_{IC} = \frac{10.627\sqrt{\frac{c}{d} + 19.646\left(\frac{c}{d}\right)^{5.5}} \cdot P}{\left(1 - \frac{c}{d}\right)^{0.25} \cdot d^{1.5}} \tag{14}$$

4. FAILURE PROCESS SIMULATION

4.1 Experimental investigation

The interpretation of results of experimental investigation on real rock is usually complicated by sample variability [2]. In order to overcome this difficulty, laboratory specimens were made from an mixture of plaster, water and retardant in a weight ratio of 1:0.2:0.005 was used to describe soft rock. Parameters of specimen are shown in Table.1 and schematic of compression test are shown in Fig.4

Table.1: Specimens` parameter

a×b×c	σ_c	σ_t	E_s	ν
mm	MPa			
100×100×10	47.4	2.5	28700	0.23

Digital Image Correlation Method (DICM) has been developed and used to measure deformation and strains of materials under various loading regimes with sub-pixel accuracy since the 1980's. It has been successfully applied to determine strains in specimens of solid and applied to a wide range of experiments.

By using this measurement, uniaxial compression test was carried out on the artificial rock-like specimens with an open hole. In fact a series of specimens were tested, the radius of open-hole increased from 5mm to 40mm at a step of every 5mm.

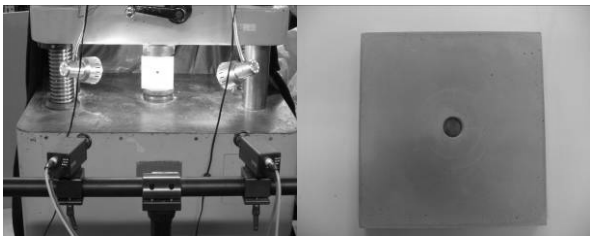

Fig.4 Schematic of compression test by using DICM and specimen with an open-hole

Due to the limitation of textual length, the strain contours of α = 20mm obtained by DICM are listed , this specimen failed at step 721, the final failure type agree well with the strain process analysis. Counter figures shows us the crack started from the edge of pre-existing defect, according to the theoretical analysis, split crack would be obtain. However due to the boundary effect, they develop in the shear zones till failure. Details are shown in Fig.5.

In order to compare the experimental conclusions, numerical simulations are also carried out.

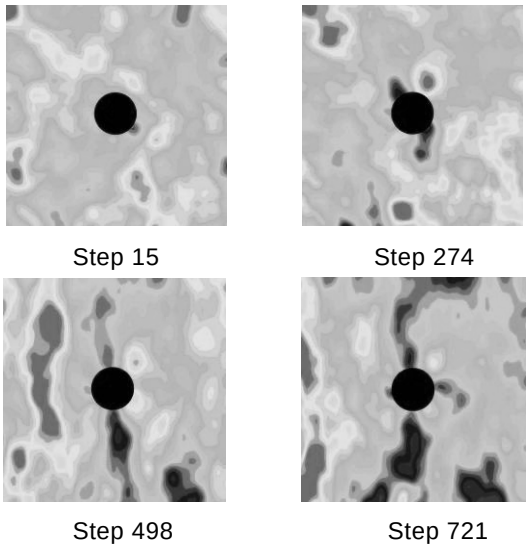

Fig.5 DICM strain contours during the test process

4.2 Numerical simulation

Numerical methods are currently the most popular method used for modeling deformation behavior of brittle solids before failure. Even though progress of failure has been obtained in numerical simulation in brittle materials, there is a lack of satisfactory models that can simulate the progressive failure of brittle solids in a more visualized way, including simulation of the failure process, failure induced seismic events and stress redistribution [10].

In this study, Realistic Failure Process Analysis code (RFPA^{2D}) is employed. Finite element technique is used in this code. The package can handle brittle material with heterogeneous material properties, and can perform non-liner deformation analysis, which includes the occurrence and development of cracks and fractures. It is a progressive damage model, which can simulate the deformation, stress distribution and failure induced stress redistribution, furthermore fracture initiation and propagation in heterogeneous materials can also be done. The consideration of heterogeneity for the elements is achieved by assigning the elements random material properties based on Weibill's distribution. Although fracture mechanics plays an important role in the analysis of defect propagation, the assumption of homogeneity adopted in fracture mechanics restricts its application in heterogeneous materials. Instead of using a fracture mechanics approach where fracture propagation is related to a stress intensity factor at the secondary crack tips and is controlled by the fracture toughness, a failure approach is adopted in the code RFPA^{2D}, where micro-fracturing occurs when the stress of an element satisfies a certain strength criterion.

Because of the grain-scale heterogeneity, the peak strength for brittle materials especially for concrete or rock can vary significantly from a local volume to another. To analyze the statistical variation of the bulk peak strength in such a heterogeneous material, Weibull (1951) adopted the statistics of extreme (Gumbel, 1958) to characterize the local failure strength by the probability distribution function

$$f(\sigma)=\frac{m}{\sigma_0}\left(\frac{\sigma}{\sigma_0}\right)^{m-1}\exp\left[-\left(\frac{\sigma}{\sigma_0}\right)^{m}\right] \qquad (15)$$

Meanwhile the cumulative probability function was given by

$$P(\sigma)=1-\exp\left[-\left(\frac{\sigma}{\sigma_0}\right)^{m}\right] \qquad (16)$$

Here the assumptions are made that the overall failure is primarily controlled by the weaker elements and that the strength of the weakest element is vanishingly small. As a consequence the statistics of failure would involve only two parameters: σ_0 and m. σ_0 is proportional to the mean value of the strength distribution, and m is a dimensionless parameter, it characterizes the degree of homogeneity in the structure. An infinitely high m value corresponds to a homogeneous structure with a uniform strength, whereas a heterogeneous structure with a broad distribution of local strength is associated with a relatively low m value [11]. In this numerical simulation, this function is applied to solve the heterogeneity of concrete, rock and rock-like materials. The value of m for our simulation is shown in Table.2.

As it is shown in Fig.6, the numerical specimens subjected to uniaxial compression. In order to determine the relationship between defect degree μ and the geometry of the specimen, each specimen is set as a mesh that consists of 100×100

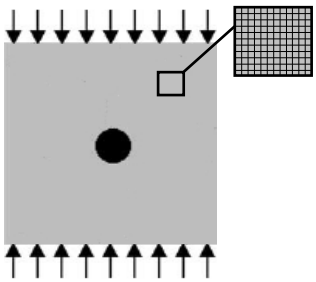

Fig.6 Schematic diagram of numerical simulation

elements (Fig. 6). Two kinds of geometry were applied in the model whose material properties are as shown in Table 2 while the geometry and radius of open-holes are as shown in Table 3.

Table 2: Parameter contained heterogeneity for numerical simulation.

	Elastic modulus (N/mm^2)	Compression strength (N/mm^2)	Poisson ratio
Average	40000	80	0.25
Heterogeneity	13	5	20

RFPA^{2D} was then used to simulate the failure process by applying a total of 180 load steps. Initially a load step of 1kN per step was applied up to 100 steps. There after a strain controlled load of about 0.001 mm per step was applied until total failure occurred.

As to the brittle materials, Mohr-Coulomb criterion has a limit on the description of tension strength. A modified coulomb failure criterion was employed in this numerical simulation. It includes tension cutoff and the tension flow rule is well associated. For details of this criterion please see, for example, Chen and Han [12].

5. RESULTS AND DISSCUTION

In this theoretical analysis and numerical simulation, there are two kinds of specimens` geometry was used, which are $100\times100mm^2$ and $150\times150mm^2$. For each of this geometry 11 of the specimens with different defect degree are established. So in total there are 22 samples are tested and calculated. The defect degree which is determined by $\mu=a/t$ is changed from 0 to 0.2 with the step of 0.02. Details are listed in Table 3:

By using the modified model, the peak strength of same samples are also calculated and compared. Fig5.a is the peak strength's comparison with the width of 100mm and Fig5.b is that of 150mm. Fracture toughness used for calculating in the modified model was obtained, according to the numerical test described above. The average value employed is $0.83MPam^{1/2}$

Table 3: Specimens` geometry

Group 1			Group 2		
a/ mm	t/ mm	μ	a/ mm	t/ mm	μ
0	50	0.00	0	75	0.00
1.0	50	0.02	1.5	75	0.02
2.0	50	0.04	3.0	75	0.04
3.0	50	0.06	4.5	75	0.06
4.0	50	0.08	6.0	75	0.08
5.0	50	0.10	7.5	75	0.10
6.0	50	0.12	9.0	75	0.12
7.0	50	0.14	10.5	75	0.14
8.0	50	0.16	12.0	75	0.16
9.0	50	0.18	13.5	75	0.18
10.0	50	0.20	15.0	75	0.20

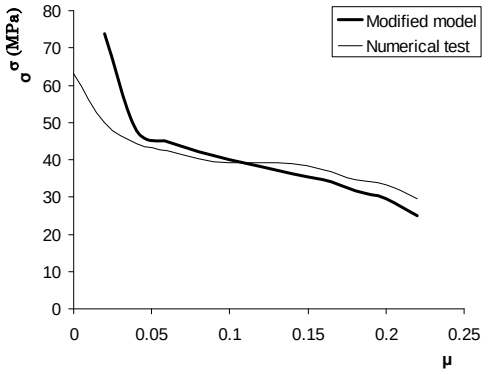

a. Peak strength of specimens with width of 100mm

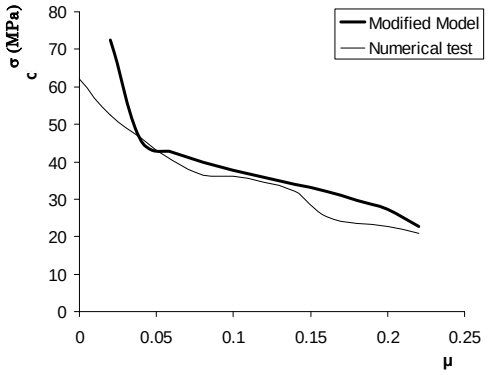

b. Peak strength of specimens with width of 150mm

Fig.7Comparison on peak strength

As it can be seen from Fig.7, both of the model and numerical simulation reveal that the peak strength reduces while the defect degree μ increasing, meanwhile μ=0.05 is the turning point, before that the peak strength of brittle specimens with an open-hole reduced quickly with the increasing of μ. The decrement of the peak strength is almost 40% of the perfect one's. After that, the rate of deceleration slows down. Moreover it shows that with the same defect degree, the wider the sample is, the weaker it becomes.

The fracture process is shown in Fig.5 as an experimental one and Fig.8 as an example of this numerical simulation. In which the peak strength is 50MPa (step151), just after that the sample fractured totally. It can be seen buckling occurs when the cracks reach the two ends of the specimen, which failure by starting a new crack in shear zones around the pre-existing open-hole. The failure mode shows that the specimen containing the smaller hole fails by cracks initiated in a shear zone connecting the hole and the surface, due to the proximity of the hole to the boundary. This failure is found to be caused by the following sequence. At first the cracks grow fast, and then, when the tips of the cracks near the ends of the specimen, the propagation slows down, or sometimes stops, due to the boundary effect.

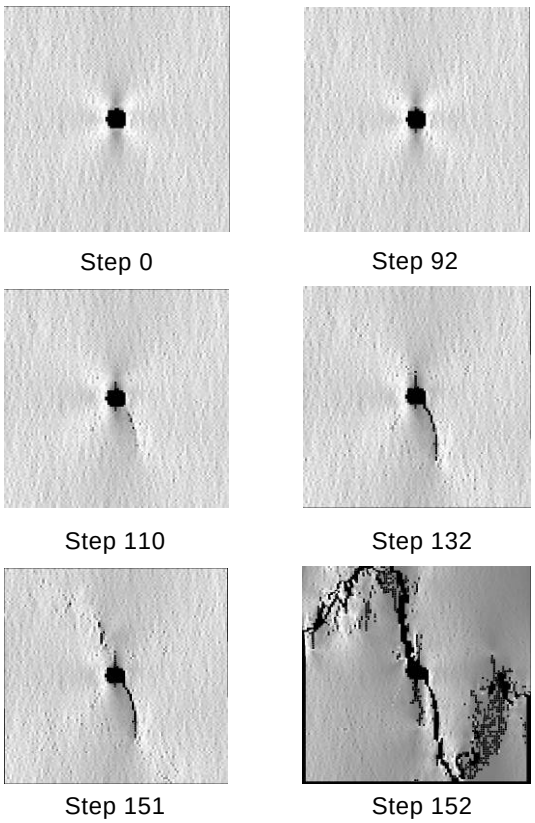

Fig.8 Numerical simulation of failure process

It is worthwhile to note that this result differs from the theoretical prediction for a hole in an infinite domain; the theoretical failure follows the split failure model. One probable reason for such differences may be due to the interaction between the growing cracks and boundary conditions, which appears to retard the crack growth as the crack is approaching the end surfaces. And, thus, the shear cracks zones are more likely to develop. That means for the brittle specimens, if the shear stress in the area between the hole and the free boundary of the specimen is high enough, shear failure will occur between the hole and the free boundary.

6. CONCLUSION

Based on the results, the following conclusions have been obtained:

1) The results of numerical simulation agrees well with the model especially $\mu > 0.05$, which means this modified model can be used for calculating the peak strength of brittle specimens with open-hole defect after the turning point.

2) Peak strength is affected by the width of sample and defect degree where peak strength decreases with the increased diameter of hole and increases with the width of sample.

3) For this study μ=0.05 is the turning point, the decrement of peak strength is almost 40% up to this turning point and after that the rate of deceleration slows down.

4) During the process simulation, the secondary cracks occur from the open-hole which agree with the theoretical analysis. However due to the boundary effect, they develop in the shear zones till failure. Therefore shear fracture model is obtained in the process simulation which can be found both in the experimental and numerical investigations.

ACKNOWLEDGEMENT

The work described in this paper was carried out at Nagasaki University, with support from

Japanese Government Scholarship. Prof. Hiroshi Matsuda and Prof. Mingrong Shen are gratefully acknowledged for many insightful discussions.

REFERENCES

[1] T. Hatano: Theory of failure of concrete and similar brittle solid on the basis of strain. International journal of fracture mechanics, Vol.**5** pp.73-92, 1969

[2] M. F. Ashby and S. D. Hallam: The failure of brittle solids containing small cracks under compressive stress states. Acta Metall. Vol. 34(3), pp.497−510. 1986

[3] E. A. George: Brittle failure of rock materials. A.A.Balkema Press. 1995

[4] C. G. Sammic and M. F. Ashby: The failure of brittle porous solids under compressive stress states. Acta Metall. Vol. 34(3), pp.511−526. 1986

[5] F. L. Matthews and R. D. Rawlings: Composite materials: engineering and science. Chapman and Hall, 1994

[6] R. H. C. Wong, C. A. Tang and K. T. Chau: Splitting failure in brittle rocks containing pre-existing flaws under uniaxial compression. Engineering fracture mechanics. Vol.69, pp.1853-1870. 2002

[7] R. W. Davidge and G. Tappin: The effective surface energy of brittle materials. Journal of materials science 3(1968), pp.165-173. 1968

[8] B. Sarit and Bhaduri: Fracture surface energy determination (110) planes in silicon by the double torsion method. Journal of materials science. Vol. 21, pp.2489-2492. 1986

[9] P. Lin, and R. H. C. Wong: Multi-crack coalescence in rock-like material under uniaxial and biaxial loading. Key engineering materials pp.183-187,809-814, 2000

[10] C. A. Tang, and R. H. C. Wong: Modeling of compression − induced splitting failure in heterogeneous brittle porous solids. Engineering fracture mechanics. Vol. 72, pp.597-615. 2005

[11] T. F. Wong, and K. T. Chau: Micro-crack statistics, Weibull distribution and micro-mechanical modeling of compressive failure in rock. Mechanics of materials. Vol.38, pp.664-681. 2006

[12] W. F. Chen, and D. J. Han: Plasticity for Structural Engineers. New York. Springers-verlag. 1988